

# Long-Term Retinal Differentiation of Human Induced Pluripotent Stem Cells in a Continuously Perfused Microfluidic Culture Device

Nima Abdolvand, Rui Tostoes, William Raimes, Vijay Kumar, Nicolas Szita, and Farlan Veraitch\*

Understanding how microenvironmental cues influence cellular behavior will enable development of efficient and robust pluripotent stem cell differentiation protocols. Unlike traditional cell culture dishes, microfluidic bioreactors can provide stable microenvironmental conditions by continuous medium perfusion at a controlled rate. The aim of this study is to investigate whether a microfluidic culture device could be used as a perfused platform for long-term cell culture processes such as the retinal differentiation of human induced pluripotent stem cells. The perfusion flow rate is established based on the degradation and consumption of growth factors (DKK-1, Noggin, IGF-1, and bFGF) and utilizing the Péclet number. The device's performance analyzed by qRT-PCR show improvements compared to the well-plate control as characterized by significantly higher expression of the markers Pax6, Chx10, and Crx on Day 5, Nrl on day 10, Crx, and Rhodopsin on day 21. Optimization of perfusion rate is an important operating variable in development of robust processes for differentiation cultures. Result demonstrates convective delivery of nutrients via perfusion has a significant impact upon the expression of key retinal markers. This study is the first continuously perfused long-term (21 days) retinal differentiation of hiPSCs in a microfluidic device.

## 1. Introduction

In 2006, Maclaren et al. demonstrated that postnatal post-mitotic photoreceptor precursors can successfully integrate into mice retina and form functional photoreceptors.<sup>[1]</sup> Since then, there has been considerable efforts to develop retinal differentiation protocols from pluripotent stem cells (PSCs).<sup>[2–11]</sup> Transplantation studies have shown that both the number

and purity of transplantable cells are crucial when it comes to increasing integration efficiency into the host retina.<sup>[12–18]</sup> Optimizing the conditions with which PSCs undergo retinal differentiation will be critical to improving the robustness, consistency, and efficacy of photoreceptor cell therapies.<sup>[19–21]</sup>

Retinal differentiation protocols for both human embryonic stem cells (hESCs) and human induced pluripotent stem cells (hiPSCs) have been developed in traditional culture formats such as T-flasks and well-plates. These formats lack the micro-environmental controls required to maintain stable culture conditions. Daily medium replacements result in fluctuations in pH, metabolites and growth factors. These short-term variations do not accurately represent the in vivo environment present during embryonic development and can adversely affect the expansion and differentiation of ESCs.<sup>[22]</sup> One solution is the adoption of perfusion bioreactors that can maintain constant concentrations of soluble factors in the liquid growth medium.<sup>[23,24]</sup>

Microfluidic devices have a number of advantages including fine spatiotemporal control over the fluid flow, small culture chambers, and the potential to run many bioreactors in parallel.<sup>[25,26]</sup> These properties make them a promising platform for investigating the best conditions for stem cell differentiation.

There are number of examples in which bespoke microfluidic culture devices have been used to study 2D differentiation processes. These include angiogenesis of mesenchymal stem cells,<sup>[27]</sup> differentiation of hESCs and hiPSCs toward mesodermal and extra-embryonic trophoblast lineage, respectively.<sup>[28,29]</sup> Others demonstrated successful culture of pluripotent stem cells under stable culture conditions<sup>[30]</sup> and long-term differentiation cultures such as, myotube differentiation of myoblasts and role of auto/paracrine factors on adipogenic differentiation of adipose-derived stem cells.<sup>[31,32]</sup>

Previously, we have developed a microfluidic culture device (MFCD) that facilitates perfused culture of standard 2D culture protocols.<sup>[33]</sup> A resalable lid allows direct manual inoculation of

Dr. N. Abdolvand, Dr. R. Tostoes, W. Raimes, V. Kumar, Prof. N. Szita, Dr. F. Veraitch  
Department of Biochemical Engineering  
University College London  
Bernard Katz building, London WC1E 6BT, UK  
E-mail: f.veraitch@ucl.ac.uk

© 2018 The Authors. *Biotechnology Journal* Published by Wiley-VCH Verlag GmbH & Co. KGaA. This is an open access article under the terms of the Creative Commons Attribution License, which permits use, distribution and reproduction in any medium, provided the original work is properly cited.

DOI: 10.1002/biot.201800323

cellular aggregates into the chamber, making the system ideal for seeding clumps of PSCs. This is especially important during directed differentiation protocols, the majority of which rely upon seeding aggregates of PSCs (known as embryoid bodies, EBs) onto 2D surfaces for extended periods with complete medium exchanges every 1–2 days. The device can be multiplexed and configured for non-invasive real-time measurements of confluency and oxygen uptake.<sup>[34,35]</sup>

The objective of this study was to investigate whether our microfluidic chamber could be applied to long-term continuously perfused cultures using retinal differentiation of hiPSCs as a case study. We used a well characterized protocol<sup>[3]</sup> and perfusion rates were decided based upon the consumption, production, and diffusion rates of four key growth factors used to induce differentiation. The onset of differentiation was monitored via the expression of key early and late stage markers revealing for the first time that a perfused microfluidic device could be used to drive the retinal differentiation of PSC. The process closely mimicked traditional well plate culture, but further investigation revealed that the perfusion rate could have a marked impact upon the expression of phenotypic markers.

## 2. Experimental Section

### 2.1. Human Induced Pluripotent Stem Cell Culture

The hiPSC line MSUH001 was obtained from Michigan State University. The cell line had been created by reprogramming the foetal female fibroblast line IMR90 via lentiviral vectors encoding the reprogramming factors Oct4, Sox2, Nanog, and Lin28. Undifferentiated hiPSCs between passage number 68 and 78 were grown on Mitomycin-C ( $1 \text{ mg mL}^{-1}$ ; Sigma-Aldrich) inactivated mouse embryo fibroblasts (MEF) in Knockout DMEM supplemented with 20% (v/v) Knockout Serum Replacement (KOSR), 1 mM L-glutamine, 1% (v/v) nonessential amino acids, 100 mM  $\beta$ -mercaptoethanol, and  $4 \text{ ng mL}^{-1}$  basic fibroblast growth factor (all Invitrogen). They were cultured in a Sanyo IncuSafe incubator at  $37^\circ\text{C}$ , and 5% (v/v)  $\text{CO}_2$ , and 10 mL of fresh medium was exchanged every 48 h. hiPSCs were transferred to newly Mitomycin-C inactivated MEF every 3–4 days with Fine Tip Mini Pastette (Alpha Laboratories).

### 2.2. Retinal Differentiation Protocol

#### 2.2.1. EB Formation

Undifferentiated hiPSCs were used to form uniform size EBs of  $\approx 1000$  cells per EB according to the AggreWell 400<sup>TM</sup> protocol. EB formation medium was prepared using DMEM/F-12 Medium (1:1) (GIBCO<sup>TM</sup>, ThermoFisher Scientific, USA), 10% (v/v) KOSR (Invitrogen, USA),  $1 \text{ ng mL}^{-1}$  Dkk-1,  $1 \text{ ng mL}^{-1}$  Noggin,  $5 \text{ ng mL}^{-1}$  IGF-1 (all R&D Systems, Minneapolis, USA), 1% (v/v) N-2 Supplement (PAA Laboratories Ltd., UK). Undifferentiated hiPSCs were detached from T-25 flasks using Tryple Express (TrypLE, ThermoFisher Scientific) and suspended as single cells in 50 mL conical tubes through a  $40 \mu\text{m}$

cell strainer (STEMCELL Technologies) to remove clumps. Flasks were rinsed with 5 mL of EB medium per millilitre of TrypLE used and were centrifuged at 300 g for 5 min at room temperature. The supernatant was removed and the pellet suspended in a small volume (1–2 mL) of EB formation medium with ROCK inhibitor (ROCKi, Y-27632). Cells were seeded at  $1.2 \times 10^6 \text{ cells mL}^{-1}$  in to each well of the AggreWell plate and incubated at  $37^\circ\text{C}$ , and 5% (v/v)  $\text{CO}_2$ . After 24 h, spent medium was exchanged for fresh medium without ROCKi and the EBs were transferred to 30 mm non-adherent bacterial grade culture dishes (Sterilin) and cultured as cell suspensions for 2 more days.

#### 2.2.2. Retinal Differentiation in Well Plates

48-well plates were used as controls for the perfusion studies. Plates were coated with 250  $\mu\text{L}$  of Matrigel (2%, BD Bioscience, San Diego, CA, USA) for 15 min and 7 EBs were transferred to each well under a dissecting microscope. The retinal differentiation medium contained DMEM/F12 (Invitrogen, US) supplemented with  $10 \text{ ng mL}^{-1}$  human recombinant DKK-1,  $10 \text{ ng mL}^{-1}$  human recombinant IGF-1,  $10 \text{ ng mL}^{-1}$  human recombinant Noggin,  $5 \text{ ng mL}^{-1}$  basic fibroblast growth factor (all R&D Systems, Minneapolis, USA), 1% (v/v) N-2 Supplement, and 2% (v/v) B27 Supplement (PAA Laboratories Ltd, UK). The operating volume was 250  $\mu\text{L}$  and spent medium was replaced once every 48 h for the duration of the differentiation protocol.

#### 2.2.3. Retinal Differentiation in Microfluidic Culture Device (MFCD)

Each MFCD was inoculated with 7 EBs and incubated overnight to allow EBs to attach to the culture surface before starting medium perfusion. Two identical MFCDs were run in parallel during the perfusion studies, one perfusing at  $130 \mu\text{L h}^{-1}$  (MFCD<sub>Hi</sub>) and the other at  $5.2 \mu\text{L h}^{-1}$  (MFCD<sub>Lo</sub>). The lower flow rate was chosen as a control to mimic the frequency of medium change in the static 48-well plates (i.e., 250  $\mu\text{L}$  per 48 h and medium height of 2.3 mm). The medium height in the MFCD<sub>Lo</sub> was adjusted by using a shallower gas permeable lid that provided a height of 2.28 mm in the culture chamber. This height adjustment allowed the fine tuning of the MFCD to as closely mimic the static control environment as possible in terms of medium exchange rate. In both perfused devices and the control culture, hiPSCs of the same batch and passage number were used at each experimental replicate.

### 2.3. Growth Factor Studies

12-well plates were used to study the degradation of DKK1, bFGF, IGF-1 and noggin at  $37^\circ\text{C}$  in differentiation medium. Plates were also inoculated with 30 EBs/well to investigate the impact of cellular consumption and production of growth factors. Where specified the medium was changed after 48 h as was described in the retinal differentiation process in well plates

above. In all conditions 1 mL of medium was used. Controls without cells were included to establish the degradation rates in differentiation medium at 37 °C. The changes in concentration of all four growth factors during the first 96 h of the EB differentiation process were investigated by taking measurements in the presence and absence of a full medium change at 48 h to observe how a scheduled medium change would affect the growth factor levels over a fixed period.

#### 2.4. ELISA

Medium samples were analyzed using sandwich ELISA kits for bFGF, IGF-1, DKK-1 (Abcam ELISA kits, Cambridge, UK) and Noggin ELISA kit (MyBioSource plc, San Diego, CA, USA). After medium collection, the cells were harvested and counted using an automated Vi-CELL Cell Viability Analyser (Beckman Coulter, Brea, CA). Each ELISA assay was performed according to the suppliers' protocol and the plates were read at 450 nm using a FLUOstar OPTIMA (BMG LABTECH GmbH, Germany) microplate reader.

#### 2.5. Microfluidic Culture Device Fabrication and Assembly

The microfluidic perfusion culture device was based on previously published designs.<sup>[33,35]</sup> In addition to the previously described design, an aluminium frame was placed around each of the two inter-connects to reinforce the top plate in order to prevent liquid from leaking (Figure 1A–D).

Connections were made using autoclavable tubing with an internal diameter (ID) of 0.8 mm and outer diameter (OD) of 1.6 mm (R1230, Upchurch Scientific, USA), along with flangeless M6 nuts (P-207, Upchurch Scientific, USA), female M6 to male Luer lock adapters (P-660, Upchurch Scientific, USA) and three-way stopcock (721664, Harvard Apparatus, UK). Syringe pumps used were KD Scientific 100 pump with 20 mL BD Plastic syringe for 130  $\mu\text{L h}^{-1}$  perfusion runs and KD Scientific, Legato 212 with 2.5 mL HSW Norm-Ject syringes for 5.2  $\mu\text{L h}^{-1}$  perfusion runs.

#### 2.6. Determination of Perfusion Rate

Based on the work of Mehta et al. in 2D modeling of microchannels, dimensionless ratio  $Pe/a$  (Equation (1)) has a determining effect in distribution of concentration in the culture area.<sup>[36]</sup>  $Pe$  is the ratio of convective transfer of a species to its diffusive transfer and it can be used to estimate whether a particular species is being carried primarily by convection or diffusion across the chamber.  $Pe/a$  value  $>1$  denotes the species of interest is delivered predominately through convection (i.e., fluid flow). In this way, Equation (1) can be used to create a quasi-steady-state concentration (excluding cell-related consumption or production) for the desired species in the culture chamber.

$$\frac{Pe}{\alpha} = \frac{Uh^2}{D_e L} \quad (1)$$

$U$  is the flow velocity,  $h$  is the channel height,  $D_e$  is diffusion coefficient of the species, and  $L$  is the channel length,  $\alpha$  is the geometric ratio ( $L/h$ ). The molecular weights of the growth factors of interest have been reported as Noggin (46 kDa), DKK-1 (25.8 kDa), IGF-1 (7.5 kDa), and bFGF (17.4 kDa). In order to estimate the diffusion coefficients of these molecules, fluorescently labelled dextrans of known molecular masses (10, 20, and 40 kDa) were used to calculate the  $Pe/a$  ratios (Table S1, Supporting Information).

#### 2.7. Immunocytochemistry

Cells were fixed with 2 mL 4% (w/v) paraformaldehyde (PFA) for 20 min at room temperature and then permeabilized with 0.3% (v/v) Triton X-100 in Dulbecco's modified phosphate-buffered saline (PBS) for 10 min at room temperature (all from Sigma-Aldrich). Samples were washed with 2 mL PBS and incubated in a blocking solution consisting of 5% (v/v) foetal bovine serum (FBS) diluted in PBS for 30 min at room temperature. Samples were incubated overnight at 4 °C with primary antibodies. The primary antibodies were all used at a dilution of 1:200. Each sample was washed with 2 mL of PBS and incubated with secondary antibody solution at room temperature for 1 hr (diluted at 1:400). Cells were washed twice with PBS before adding a solution of 4,6-diamidino-2-phenylindole (DAPI; Invitrogen; diluted at 1:1,000) and incubated for 5 min at room temperature before one final wash with PBS. Fluorescent images were acquired using Nikon's Eclipse TE2000-U and Life Technologies' EVOS<sup>®</sup> FL fluorescence microscopes. Complete list of primary and secondary antibodies used provided in Table S2, Supporting Information.

#### 2.8. Quantitative RT-PCR

##### 2.8.1. RNA Extraction

RNAs were extracted using the Qiagen RNeasy kit (Qiagen, Crawley, UK) as directed by manufacturer's protocol. The RNA concentration was determined by measuring absorbance at 260 nm, by spectrophotometer (NanoDrop ND-1000, Thermo Scientific, Epsom, UK).

##### 2.8.2. cDNA Synthesis

The concentration of each RNA sample was normalized to undifferentiated hiPSC before synthesising cDNA using the QuantiTect Whole Transcriptome Kit (Qiagen, Crawley, UK). Amplified cDNAs were stored at  $-20^\circ\text{C}$  before use in the next step.

##### 2.8.3. qPCR

Quantitative polymerase chain reactions (qPCRs) were performed by using the MESA BLUE qPCR MasterMix Plus

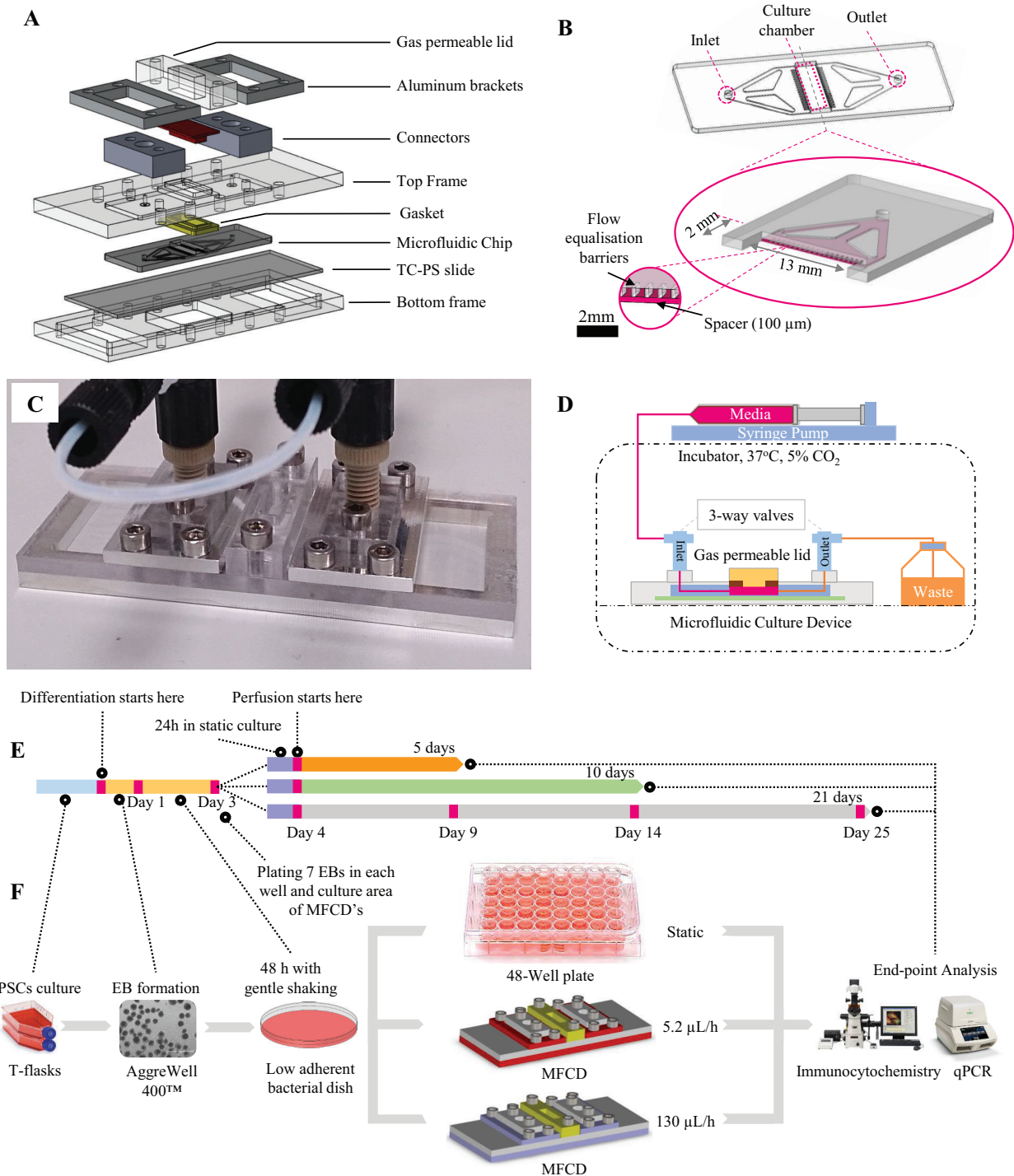


**Figure 1.** A) Exploded view of the microfluidic culture device. B) Microfluidic chip, inlet and outlet channels, culture chamber, and their dimensions. C) Image of the assembled microfluidic culture device with aluminium frames. D) Schematic representation of the perfusion set-up with syringe pump kept outside of the incubator. E) Process timeline from hiPSCs culture to end-point analysis of the cells. The upper side of the line includes the specific steps, and the lower side shows the timing of each process. F) Schematics representation of each process step. The stepwise process of retinal differentiation was initiated by formation of the EBs using AggreWell 400™, followed by a 2-day culture of the EBs with gentle shaking in low adherent bacterial dish. 7 EBs were transferred into one well of 48-well plate and culture area of each MFCD coated with Matrigel for the retinal determination step. Following a 24-h static incubation for attachment of the cells to the culture area the perfusion cultures were initiated at two flow rates of 130 and 5.2  $\mu\text{L h}^{-1}$ , respectively. The lower flow rate of 5.2  $\mu\text{L h}^{-1}$  provides similar medium height and identical medium exchange to the 48-well plate control, providing a second control for the MFCD with the higher flow rate. Expression of the retinal markers was analyzed using immunocytochemistry and qPCR.

for SYBR Assay (Eurogentec, Hampshire, UK) following the manufacturer's instructions. Primer pairs for the target and housekeeping genes,  $\beta$ -actin, UBC, Oct4, Sox2, Nanog, Nesting, Sox17, Brachyury, Otx2, Pax6, Lhx2, Six6, Vsx2/Chx10, Crx, Nrl and Rhodopsin were all acquired from Qiagen (Qiagen, Germany, Table S3, Supporting Information). Triplicates were run for each sample and all samples were normalized to levels of  $\beta$ -actin and UBC expression in hiPSCs. hiPSCs were used to act as a calibrator between the time points.

## 2.9. Statistical Analysis

All cell culture experiments were conducted as biological triplicates ( $n = 3$ ). Data points are presented as the mean of three repeats, and error bars represent SEM.  $p < 0.05$  was considered to be significant, indicated in the figures by an asterisk (\*). When comparing means of two paired groups, a two-tailed, paired  $t$ -test was used. In order to find significant differences of gene expression between flow rates and the control, a one-way repeated ANOVA was used followed by Tukey's post-hoc multiple comparisons test.

## 3. Results

### 3.1. Characteristics of the Microfluidic Culture Device

The modular design of the MFCD was comprised of a gas permeable lid made from poly(dimethylsiloxane) (PDMS) and a lid holder from polycarbonate (PC), two interconnects made of PC, a top frame (PC), bottom frame and reinforcement brackets made from Aluminium (Al), a gasket and a microfluidic chip made from PDMS, and a tissue-culture polystyrene (TC-PS) slide as a culture surface, mirroring the same culture surface as conventional cell culture dishes. The cassette-like design allowed for replacement of the individual parts when necessary, reducing time and fabrication costs compared to single-use devices. All parts were autoclavable, and gas permeable parts allowed sufficient aeration to the culture chamber. The MFCD was primed by circulating the media via three-way valves through the inlet and outlet of the device to remove any trapped bubbles prior to seeding the EBs. The fresh media was perfused through the device via a syringe connected to a syringe pump placed outside the incubator and kept on ice-packs for the duration of the experiments (Figure 1D). The microfluidic chip was designed such that housed a  $0.52 \text{ cm}^2$  culture area providing a uniform flow by use of  $200 \mu\text{m}$  deep flow channels connecting the inlet and outlet ports to the culture chamber. Furthermore, it provided a very low mean hydrodynamic shear stress of  $1.33 \times 10^{-4} \text{ Pa} \pm 0.37 \times 10^{-4} \text{ Pa}$  (calculated by computational fluid dynamics modelling) at the height of  $10 \mu\text{m}$  above the culture surface at a flow rate of  $300 \mu\text{L} \cdot \text{h}^{-1}$ .<sup>[33]</sup> This avoids adverse effects of the hydrodynamic shear stress on cellular processes, making it an ideal device for the study of convective delivery of nutrients on differentiation cultures. Figure 1E,F shows the process flow chart for the retinal differentiation of hiPSCs in our microfluidic device.

### 3.2. Growth Factor's Dynamics During Retinal Differentiation of hiPSCs

The degradation, consumption, and production of the four key growth factors involved in the retinal differentiation process of hiPSCs were investigated in order to establish a perfusion rate for the differentiation process.

During cell-free experiments DKK-1 was shown to degrade most rapidly and was reduced to only 48% of its initial concentration in an 8 h period (Figure 2A). There was also degradation of bFGF and Noggin (Figure 2B,C) resulting in concentration drops of 69 and 46%, respectively, relative to their initial concentrations, within the first 24 h. IGF-1 was stable at  $37^\circ\text{C}$  (Figure 2D).

In the presence of differentiating hiPSCs DKK-1 levels dropped rapidly from  $5.27 \pm 0.23 \text{ ng mL}^{-1}$  to  $2.53 \pm 0.25 \text{ ng mL}^{-1}$  within the first 8 h (Figure 2A). DKK-1 concentration decreased a further 12% between 8 and 24 h where it remained steady before the medium exchange at 48 h. After exchanging the medium, the decrease in concentration followed a similar trend. However, there was a clear increase in DKK-1 concentration between 72 and 96 h post medium change indicating that the cells may have started secreting the growth factor during this later period (Figure S1, Supporting Information).

The concentration of bFGF remained high in cultures at  $4.23 \pm 0.71 \text{ ng mL}^{-1}$  for both with and without medium exchange (Figure 2B). Since degradation studies showed degradation of bFGF by 69% within the first 24 h, we concluded that the cells were producing bFGF (Figure S1B, Supporting Information).

Noggin and IGF-1 concentrations decreased during the first 24 h from  $4.84 \pm 0.24$  and  $6.56 \pm 0.35 \text{ ng mL}^{-1}$  down to  $0.82 \pm 0.41$  and  $3.53 \pm 0.29 \text{ ng mL}^{-1}$ , respectively, before remaining steady until the medium change at 48 h (Figure 2C,D). After the medium change the concentration of both growth factors dropped rapidly within the first 4 h before then plateauing for the remainder of the culture period.

### 3.3. Determination of Perfusion Rate for Convective Delivery of Nutrients

The ratio  $Pe/a$  was used to determine the minimum flow rate required for delivering growth factors of interest in retinal differentiation medium. Figure 2E shows that a flow rate of  $650 \mu\text{L h}^{-1}$  is required to have bFGF, Noggin, and DKK-1 in primarily convective delivery. A flow rate of  $130 \mu\text{L h}^{-1}$  is required to have DKK-1 and Noggin in convection and  $100 \mu\text{L h}^{-1}$  for only Noggin to be in predominately convective flow. IGF-1 has a molecular weight of 7.5 kDa, which requires a flow rate of more than  $650 \mu\text{L h}^{-1}$  to be delivered to the cells by convection. Based on the high degradation rate of DKK-1, the high consumption rate of Noggin and the importance of both growth factors as confirmed in an independent study<sup>[5]</sup> we decided to use a flow rate of  $130 \mu\text{L h}^{-1}$ . At this flow rate both of these key growth factors would be delivered to the cells via convection maintaining a steady concentration as the cells differentiate.

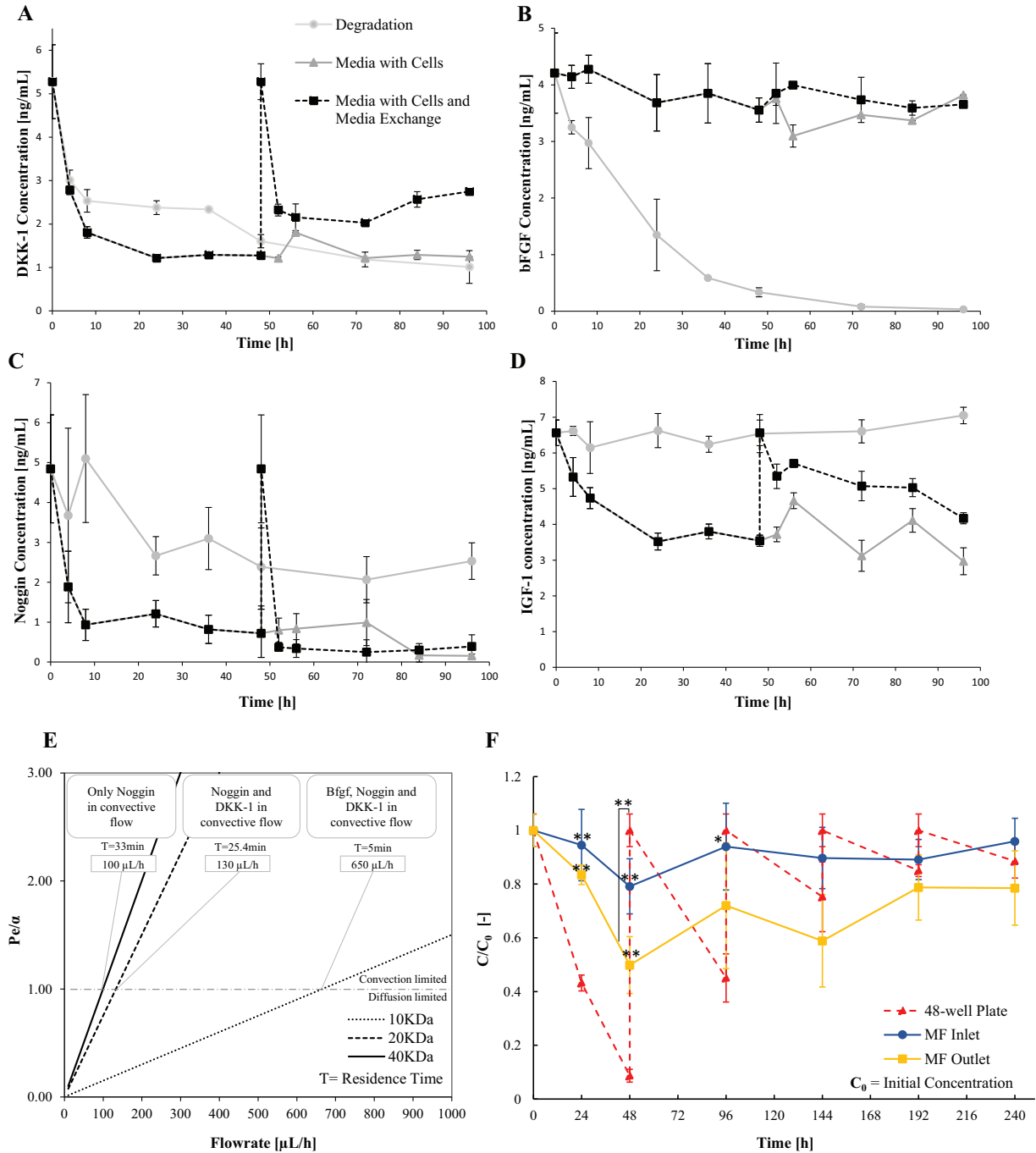


**Figure 2.** Degradation and Consumption Profile of (A) DKK-1, (B) bFGF, (C) Noggin, and (D) IGF-1 over the course of 96 h. Experiments performed in 12-well plates using 30 EBs per well. ELISA was used as the method of analysis. Error bars represent one SEM about the mean of three independent data points ( $n = 3$ ). E) Showing critical perfusion rate for convective delivery of species using Péclet Number.  $Pe/a > 1$  represents the convective delivery of the species by fluid flow to the cells and  $Pe/a < 1$  denotes the diffusive delivery of the molecules. The intersection of the representative lines with the  $Pe/a = 1$  shows the minimum required flow rate for having the molecules of that weight (and higher) in convective delivery mode. (F) DKK-1 Concentration in MFCD over 10 days' retinal differentiation of hiPSCs at the inlet and outlet of MFCD compared to the 48-well plate control. Error bars represent one SEM about the mean of three independent data points ( $n = 3$ ) (\* $p < 0.05$ ; \*\* $p < 0.01$ ). A repeated measures ANOVA indicated a significant difference in the expression of each gene between the three conditions. To establish significance of the difference between the conditions, a Tukey's post-test was applied.

### 3.4. Stable Concentration of DKK-1 in Microfluidic Culture Device

In order to confirm that a perfusion rate of  $130 \mu\text{L h}^{-1}$  was sufficient to deliver constant concentrations of the most unstable growth factors we measured the concentration of DKK-1 (MW 25.8 kDa) at the inlet and outlet of the MFCD (Figure 2F). EBs were formed via centrifugation using AggreWell 400™ plates and allowed to mature in suspension before being seeded directly into the microfluidic chamber. Once inoculated the device was run in static mode for 24 h to allow the EBs to attach before switching to perfusion mode.

During the differentiation process in the 48-well plate control, the concentration of DKK-1 fluctuated from initial concentration of  $5.51 \pm 0.81 \text{ ng mL}$  down to  $0.47 \pm 0.24$ ,  $2.48 \pm 0.16$ , and  $4.14 \pm 0.73 \text{ ng mL}$  at 48, 96, and 144 h, corresponding to the complete medium changes which were performed every 48 h. These fluctuations became less and less pronounced reaching to values of  $4.90 \pm 0.64$  and  $4.91 \pm 0.83 \text{ ng mL}$  as the differentiation process progressed until day 10. In the continuously perfused MFCD there was a significant ( $p < 0.001$ ) drop in DKK-1 when comparing the inlet and outlet concentrations at 24 and 48 h. This implies that cells were indeed consuming DKK-1 as it passed through the chamber. The DKK-1 concentration in the MFCD at the outlet shows a 45% reduction in concentration of this factor within the first 48 h of perfused culture as compared with a 90% drop in 48-well plates.

### 3.5. Morphological Analysis of the Cultures During Retinal Differentiation

In subsequent differentiation experiments the microfluidic device was perfused at two flow rates.  $130 \mu\text{L h}^{-1}$  (MFCD<sub>Hi</sub>) and a lower flow rate of  $5.2 \mu\text{L h}^{-1}$  (MFCD<sub>Lo</sub>) were run in parallel to investigate whether the process was improved by lower flow rates which may allow the accumulation of secreted factors.

The initial 24 h incubation in static prior to starting perfusion allowed EBs to partially expand and adhere to the surface. During this period EBs maintained their 3D structure where gradual spreading of the cells outward from the core of the EBs formed a unicellular layer on the periphery and a dense multi-layered core during the first 4–5 days in all cases (Figure 3A,C). There was no morphological evidence on reaction of the cells to the perfusion during the course of experiments. Multi-layered structures formed throughout the culture period in all three conditions. Neural rosettes appeared between days 5–6 in the 48-well plates controls and disappearing on day 8–9. The rosettes were not observed in the MFCD<sub>Hi</sub> (Figure 3D–F). In the MFCD<sub>Lo</sub> the neural rosettes had a delayed appearance compared to the 48-well plates control. They were observed on days 8–9, and stayed for a longer period before disappearing between days 12–14 (Figure 3M–R). In the 48-well plate controls, EBs tended to aggregate in the centre of the culture area, creating a denser population in the middle before spreading throughout the culture area (Figure 3G).

In the MFCD<sub>Hi</sub> uniform expansion was observed with fewer 3D like structures. The EBs expanded in monolayers early during

differentiation before growing into multi-layers later on. After day 10, cells exhibited a higher degree of homogeneity compared to the other cultures (Figure 3C, F, I, L). In the MFCD<sub>Hi</sub>, sheets of hexagonal cells morphologically similar to early RPE cells, (without any pigmentation commonly observed in mature RPEs) were observed between days 10 and 12 (Figure 3K). These cellular layers disappeared after a period of 4–5 days.

### 3.6. Expression of the Retinal Progenitor Markers

In order to investigate whether the differentiation was occurring, MFCD and control cultures were stained for a panel of retinal lineage markers. Both perfused cultures as well as the static control culture exhibited positive expression of early neuroectoderm markers, Nestin and Otx2 after 5 days. After 10 days, the expression of eye-field transcription factor (EFTF), Pax6, and optic vesicle (OV) marker, Vsx2/Chx10, was observed across all culture formats. Expression of photoreceptor precursors markers, Crx and Nrl were observed on day 21 of culture (Figure 4A,C).

### 3.7. Improved Gene Expression in Perfused Cultures

qPCR was undertaken to study the effect of the MCFD and flow rate on the expression of pluripotency, retinal, and germ layer markers. The first 5 days of culture revealed an expected downregulation of pluripotency markers Oct4, Nanog, and Sox2 as cells began to differentiate. As differentiation progressed there was continued downregulation of Oct4 and Nanog with no significant differences between the MCFDs and 48-well plate controls (Figure 5A,B). After an initial downregulation of Sox2 expression, a rise was evident in all cultures apart from the MFCD<sub>Lo</sub> after day 5 (Figure 5C).

Figure 5D Shows upregulation of Nestin (ectoderm) during the course of differentiation across devices. There was no significant difference between different culture formats. Expression of an early mesoderm (Brachyury) and an early endoderm (Sox17) markers were investigated to determine the extent to which the differentiation in the MCFD would be directed into lineages not capable of differentiating into neural retinal cells. There was a small increase in the expression of both genes during the first 5 days in all three conditions after which they were downregulated. After 21 days of differentiation the highest expression of Brachyury was in the MFCD<sub>Hi</sub> while the highest expression of Sox17 was observed in the MFCD<sub>Lo</sub> (Figure 5E,F).

In terms of early retinal marker expression, the expression of Otx2 increased most rapidly between day 5 and 10 in the 48-well plate control (Figure 5G). On day 5, Pax6 expression was highest in the MFCD<sub>Lo</sub> ( $p < 0.05$ ). On day 21, Pax6 expression in the MFCD<sub>Lo</sub> was significantly lower than the control ( $p < 0.05$ , Figure 5H). On day 21, upregulation of Six6 peaked in the MCFDs with a significant difference between the MFCD<sub>Lo</sub> and MFCD<sub>Hi</sub> ( $p < 0.05$ , Figure 5I). There was no significant difference in the expression of Lhx2 between all three conditions and they all showed steady increase in expression of this marker during the 21 day period (Figure 5J).

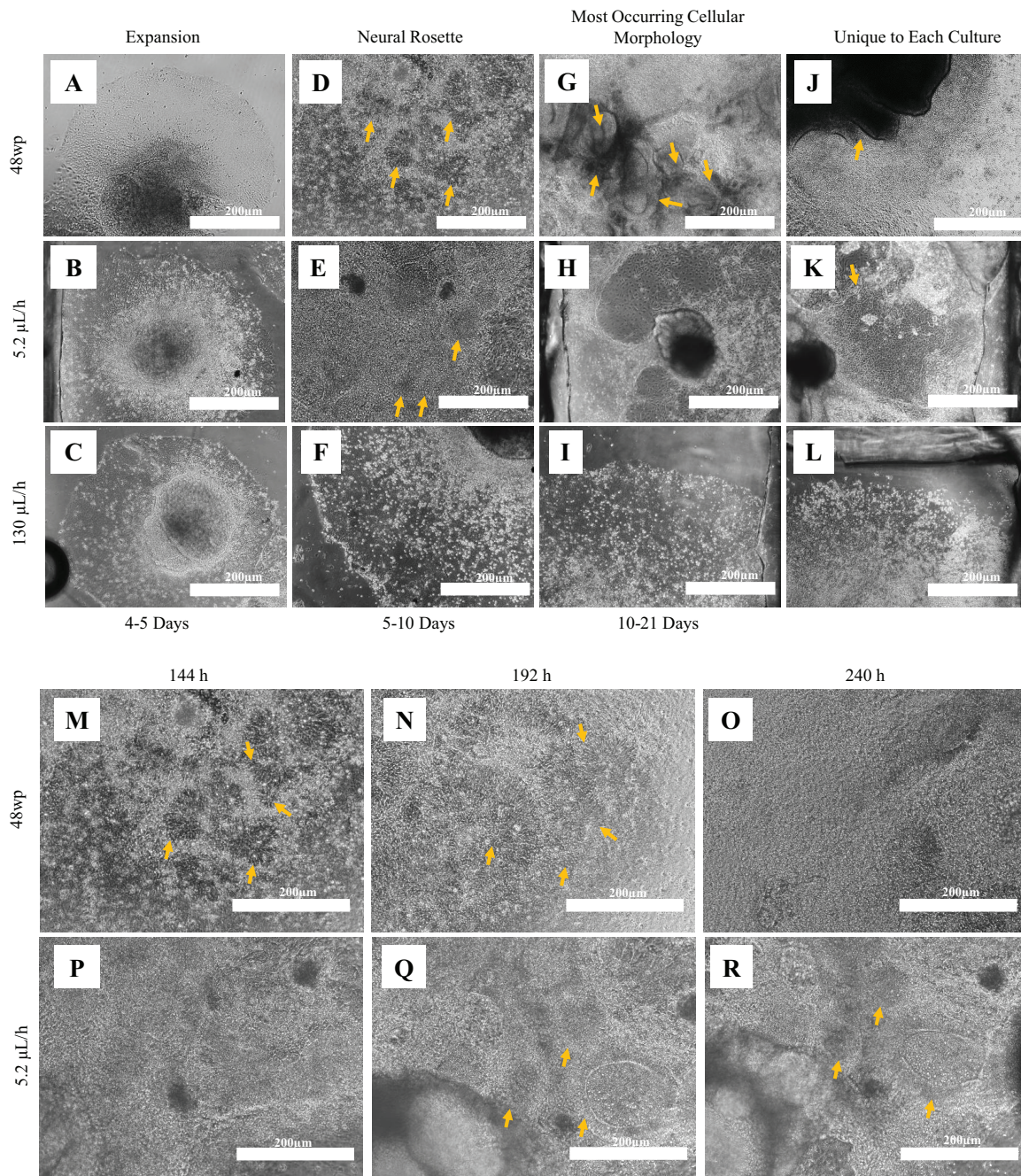


**Figure 3.** A–L) EBs expanded in a similar fashion across all devices during the first 4–5 days of the culture. MFCD<sub>Lo</sub> typically exhibited a monolayer expansion of cells and larger amount of cellular debris. MFCD<sub>Hi</sub> presented a more uniform expansion of the cells, especially between day 10 and 21. One of the exclusive features that appeared among the cultures in MFCD<sub>Lo</sub> were formation of the polygonal RPE like cells around days 10–12 of the culture. M–R) Neural rosettes are typically formed around days 5–7 in the control cultures before disappearing on days 8–9. In MFCD<sub>Lo</sub>, they appeared on day 8–9 and stayed longer before they disappeared on days 12–14. Neural rosettes did not appear in the MFCD<sub>Hi</sub>.

Vsx2/Chx10 is a transcription marker associated with the formation of retinal stem cells capable of differentiating into retinal neurons.<sup>[37]</sup> It exhibited a rapid increase in expression on day 5 of differentiation in the MFCD when compared with the 48-well plate control ( $p < 0.01$ ). The most rapid increase in expression of Vsx2/Chx10 was observed in the MFCD<sub>Lo</sub> which

was significantly higher than in the MFCD<sub>Hi</sub> ( $p < 0.01$ ). For the remainder of culture period, there were no other significant differences in the expression of Vsx2/Chx10 between any conditions, however further upregulation was evident at subsequent time points with the exception of the MFCD<sub>Hi</sub> on day 21 (Figure 5K).



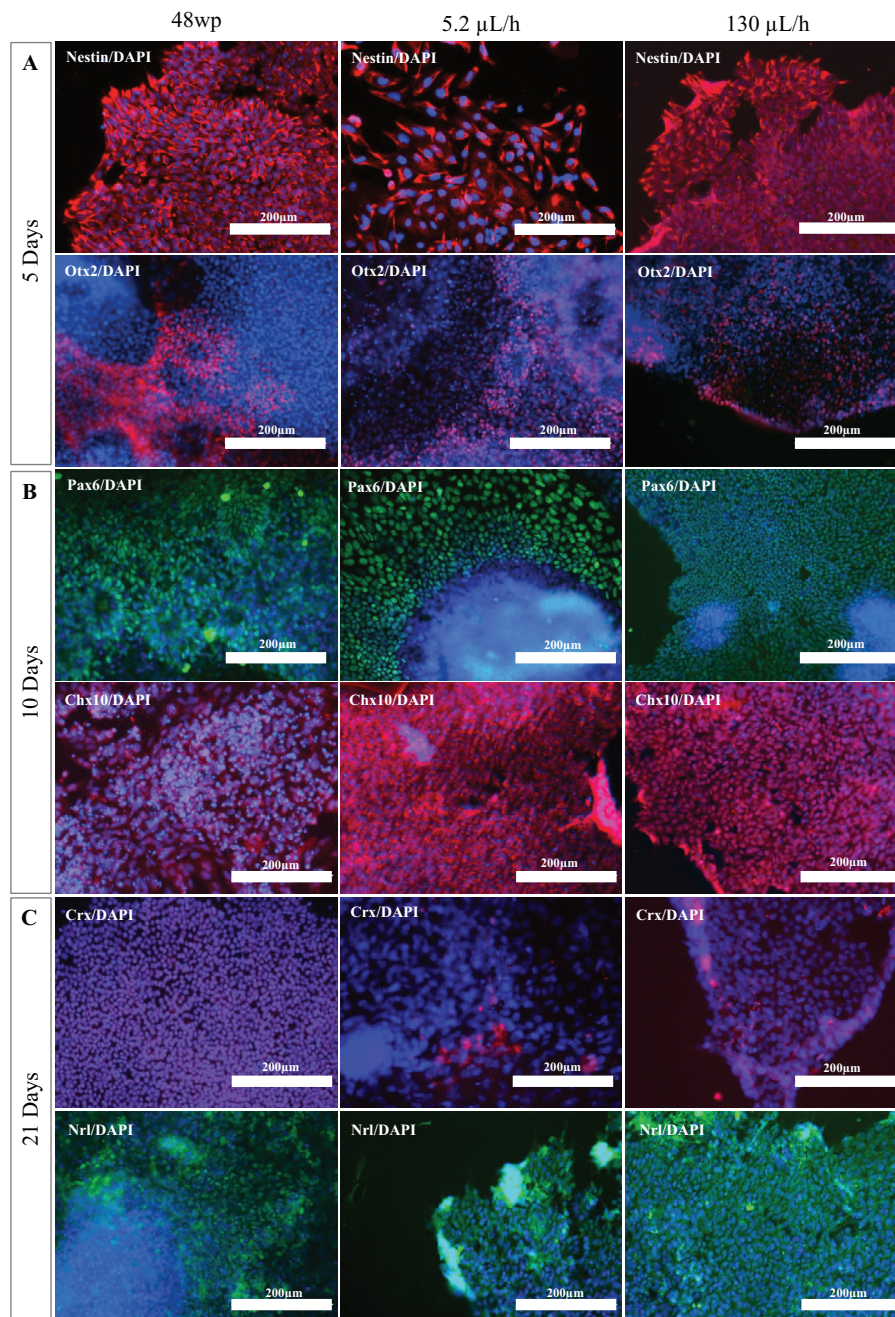


**Figure 4.** A) Shows positive expression of Nestin and Otx2 on day 5 of the culture. B) Showing positive expression of the markers Pax6 and Vsx2/Chx10 across all culture devices on day 10. C) Showing positive expression of the retinal precursor markers Crx and Nrl across all culture devices on day 21.

Crx and Nrl have previously been shown to be key markers of regenerative photoreceptor precursors capable of translocating to the retina and differentiating into functional photoreceptors upon transplantation into the sub-retinal space.<sup>[1]</sup> The expression of Crx was significantly higher in the MFCDs on day 5 when compared to the 48-well plate controls ( $p < 0.05$ ). Its expression continued to rise until the end of the culture period and after 21 days there was significantly more Crx expression in the MFCD<sub>Hi</sub> ( $p < 0.05$ ). Both MFCD

conditions expressed higher levels of Crx than in the 48-well plate control (Figure 5L). The expression of Nrl peaked at day 10 and plateaued for the rest of the differentiation in the control cultures. The highest expression of Nrl ( $p < 0.01$ ) was observed in the MFCD<sub>Lo</sub> at day 10. Extended culture in the MFCD at both flow rates was associated with the down-regulation of Nrl expression and after 21 days there was comparable levels of this key transcription factor in all three cultures (Figure 5M).

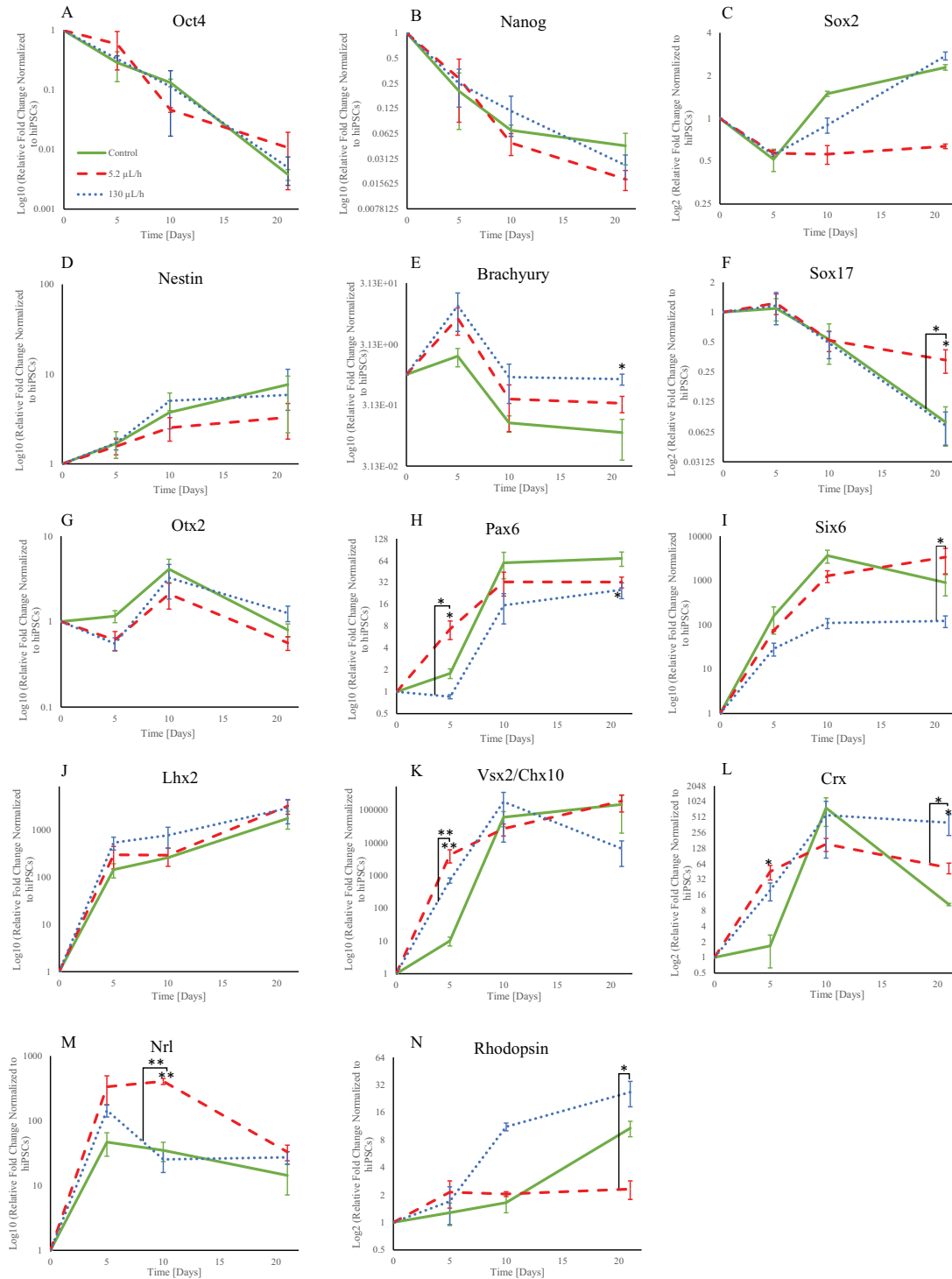


**Figure 5.** Shows down-regulation of the pluripotency markers (A) Oct4, (B) Nanog, and (C) Sox2 across the different culture formats. Expression of different germ layer markers (D) Nestin (ectoderm), (E) Brachyury (mesoderm) and (F) Sox17 (endoderm). EFTFs in (G) Otx2, (H) Pax6, (I) Six6, and (J) Lhx2. Optic vesicle marker (K) VSx2/Chx10 and retinal precursor markers (L) Crx and (M) Nrl. (N) Shows expression of Rhodopsin. Error bars represent one SEM about the mean of three independent data points ( $n = 3$ ) (\* $p < 0.05$ ; \*\* $p < 0.01$ ). A repeated measures ANOVA indicated a significant difference in the expression of each gene between the three conditions. To establish significance between different conditions, a Tukey's post-test was applied.

Rhodopsin, a receptor protein found on the surface of rod cells,<sup>[38]</sup> was used to characterize late stage differentiation in the MFCDs. At the end of the culture period the expression of Rhodopsin was very similar in the MFCD<sub>Hi</sub> and the 48-well plate control. Differentiation under lower flow rates lead to significantly ( $p < 0.05$ ) lower levels of Rhodopsin expression indicating that there may be a minimum flow rate needed to effectively differentiate hiPSCs into mature photoreceptor cells (Figure 5N). Overview of the average expression of different markers throughout retinal differentiation of hiPSCs have been summarized in Figure S2, Supporting Information.

#### 4. Discussion

The goal of this study was to establish a process for the retinal differentiation of hiPSCs in a microfluidic cell culture device. The microfluidic culture device had been designed specifically for regenerative medicine process development and enabled greater control over the cellular microenvironment with regards to shear stress and transport of soluble factors. The MFCD has previously been used to successfully expand hESCs and mESCs<sup>[33–35]</sup> meaning that this was the first attempt to undertake a lengthy directed differentiation process. The modular design of the MFCD was advantageous for the simple implementation of stepwise differentiation protocols. The lid design meant that EBs could be directly seeded into the culture chamber, thus avoiding the flow through seeding and/or specialized arrangements for in-situ EB formation. hiPSCs could be aggregated into EBs using standard techniques (in this case Aggrewell 400<sup>TM</sup>) and directly pipetted into the cell culture chamber. The modular design also allowed for easier and more efficient collection of cells at the end of the process for qPCR and immunocytochemistry.

In order to determine the appropriate perfusion rate for differentiation, a number of considerations were taken into account. Perfusing at low flow rates can limit the mass transfer of nutrients and growth factors resulting in the accumulation of waste products over time. Higher flow rates can introduce shear stresses and risk of cellular washout. Specially designed fluidics have been employed to minimize the exposure of attached cells to excessive shear rates in our MCFD.<sup>[33]</sup>

In order to determine which growth factors were of greatest importance to the differentiation process it was necessary to examine the cellular demands, stability and rates of production/consumption. The Péclet number calculations for each growth factor showed that there is a perfusion rate threshold which allows for convective delivery to be dominant.

Degradation studies revealed that DKK-1 and bFGF degraded the fastest at 37 °C and should be delivered primarily by convection to the cells. Further investigation of growth factor production rates during standard cell culture revealed that bFGF was being produced by the cells meaning that it was not necessary to supply this factor by convection. Noggin, IGF-1 and DKK-1 had the highest demand in the first 48 h of the culture. (Figure S1, Supporting Information) IGF-1, being the smallest molecule of the group, requires a flow rate of more than 650  $\mu\text{L}\cdot\text{h}^{-1}$  in order to be delivered primarily by convection in the MFCD. This flow rate would be too high resulting in the other

growth factors being forced out of the chamber before they diffuse sufficiently through the medium and have the opportunity to be delivered to the cells. In addition, IGF-1 is more resistant to degradation than all the other growth factors and the functional importance of DKK-1 and Noggin during photoreceptor differentiation has been confirmed by a second group.<sup>[5]</sup> As a result we selected a flow rate of 130  $\mu\text{L}\cdot\text{h}^{-1}$ , which meant that DKK-1, Noggin and other molecules such as B27 and N2 supplements, BSA and transferrin were delivered primarily via convection.

Morphological evaluation of the cultures showed clear similarities as well as some distinct differences between each of the cultures. The mean calculated hydrodynamic shear stress reported in our MFCD was  $1.33 \times 10^{-4} \text{ Pa} \pm 0.37 \times 10^{-4} \text{ Pa}$  at the height of 10  $\mu\text{m}$  above the culture surface at a flow rate of 300  $\mu\text{L}\cdot\text{h}^{-1}$ .<sup>[33]</sup> This rate is three orders of magnitude lower than what Toh et al.<sup>[39]</sup> observed in mESCs,  $4.5 \times 10^{-1} \text{ Pa}$  for negative effects of the shear and an order of magnitude lower than  $1.6 \times 10^{-3} \text{ Pa}$ , for expression of *fgf5* in the same cell population, indicating the effect of shear on the genetic level. For cells to experience the shear stress of  $1.6 \times 10^{-3} \text{ Pa}$  in our MFCD a flow rate of 3600  $\mu\text{L}\cdot\text{h}^{-1}$  is required. Whereas, in these experiments, flow rate of 130  $\mu\text{L}\cdot\text{h}^{-1}$  was used, which was less than half of what has been reported previously by Reichen et al. Furthermore, no morphological changes were observed during the course of experiments to indicate any negative effects of the shear by the cells. However, a more in-depth analysis of the cells such as expression of *fgf5* may reveal the possible effect of shear at this flow rate.

Differences observed in MFCD<sub>Lo</sub> could have been due to the  $Pe/\alpha < 1$  in this culture. Under these conditions the provision of growth factors is dominated by diffusion and may result in depletion over time. Also, accumulating waste molecules would be removed at a slower rate compared to the control and the MFCD<sub>Hi</sub>. Morphological observation in the MFCD<sub>Hi</sub>, indicates possible wash-out of the exogenous molecules that contribute to the formation of neural rosettes, which were present both in control culture (48wp) and MFCD<sub>Lo</sub>. Neural rosettes are often present during the early retinal differentiation of hESCs and hiPSCs in the presence of IGF-1.<sup>[3]</sup> IGF-1 has been shown to be crucial during the formation of retinal progenitors.<sup>[40]</sup> MFCD<sub>Hi</sub> also showed a more homogeneous population of the cells and less formation of the 3D structures, which could have been due to the higher removal rate of waste molecules or endogenous signalling factors from the culture area by perfusion. Formation of the RPE like cells could have been linked to higher expression of the marker *Vsx2/Chx10*. It has been reported that *Vsx2/Chx10* expression affects expression of the marker *Mitf* in the RPE cells. Suppression of the marker *Mitf*, induces differentiation of optic vesicle cells toward retinal progenitor cells.<sup>[41]</sup>

Differences in morphology did not necessarily coincide with the expression of certain genes in these cultures. Although the down regulation of pluripotent markers was unaffected, the perfusion rate had a marked affect upon the expression of germ layer markers. After 21 days of differentiation MFCD<sub>Hi</sub> was associated with the highest persistence of mesodermal marker *Brachyury* while there was significantly more expression of endoderm marker *Sox17* in MFCD<sub>Lo</sub>. Significant expression of the mesodermal and endodermal markers at the late stages of

retinal differentiation may have a less significant effect on the homogeneity of the culture. However, since expression of both of these markers are undesirable for retinal differentiation, further investigation is required to establish a flow rate/regime that could mitigate expression of such unwanted markers.

Overall, significantly higher expression of Vsx2/Chx10, Crx and Nrl was observed in both perfused devices on days 5 and 10 compared to the control culture. Retinal progenitors committed to become photoreceptors express Crx as well as mature photoreceptors. Expression of Crx indicates higher number of photoreceptor in the cell population.<sup>[42]</sup> Nrl expression results in development of cone photoreceptors.<sup>[43]</sup> It was reported previously that post-mitotic precursors that express both Nrl and Crx have the highest chance of successful integration into host tissue post-transplantation.<sup>[1,15]</sup> In humans Rhodopsin is expressed mostly at late stages of photoreceptor maturation around weeks 10–15.<sup>[21]</sup> Considering 3 weeks differentiation of the cells, comparable expression of this marker was observed in MFCD<sub>Hi</sub> and well-plate control culture, which could have been due to its lower expression at this time point. However, differences between the perfused devices was of note here, indicating the unfavorable condition at low flow rate cultures for this marker.

## 5. Conclusions

We have demonstrated the longest continuous differentiation of hiPSCs in a microfluidic culture device to date by successfully maintaining cultures for 21 days in continuous perfusion. Executing long, complex, differentiation processes such as this, in a microfluidic chip, under continuous perfusion is a significant technical advancement. This study represents a significant step forward towards the application of microfluidic technology to pluripotent stem cells in the fields of developmental biology, disease modelling and regenerative medicine process development.

Measurements for DKK-1 showed that the concentration of this growth factor must be adapted to the cellular needs during the course of differentiation. An interesting observation was the impact of convective delivery of the key growth factors via perfusion on the expression of key retinal progenitor markers, Pax6, Vsx2, and Crx suggesting that flow rate is a key parameter which warrants further investigation. Optimization of perfusion rate may prove to be an important operating variable as we move toward clinical application and robust processes which require fine control over differentiation. Degradation, consumption, and endogenous expression of the key growth factors are vital when deciding the most suitable and cost-effective protocol for perfused cultures.

## Supporting Information

Supporting Information is available from the Wiley Online Library or from the author.

## Acknowledgments

The authors would like to acknowledge the Engineering and Physical Sciences Research Council (EPSRC, EP/ I005471/1) for funding of the microfluidic device development.

## Conflict of Interest

The authors declared no potential conflicts of interest with respect to the research, authorship, and/or publication of this article. A patent application has been filed by UCL Business, a wholly owned subsidiary of UCL (www.uclb.com). The application number is PCT/GB2009/002778. The author Nicolas Szita may become potential beneficiaries of that patent application in the future. There are no further products in development or marketed products to declare.

## Keywords

cell culture, microfluidic culture device, microbio reactor, process development, stem cells, retinal differentiation

Received: June 1, 2018

Revised: August 15, 2018

Published online:

- [1] R. E. MacLaren, R. A. Pearson, A. MacNeil, R. H. Douglas, T. E. Salt, M. Akimoto, A. Swaroop, J. C. Sowden, R. R. Ali, *Nature* **2006**, *444*, 203.
- [2] M. Eiraku, N. Takata, H. Ishibashi, M. Kawada, E. Sakakura, S. Okuda, K. Sekiguchi, T. Adachi, Y. Sasai, *Nature* **2011**, *472*, 51.
- [3] D. A. Lamba, M. O. Karl, C. B. Ware, T. A. Reh, *Proc. Natl. Acad. Sci. USA* **2006**, *103*, 12769.
- [4] J. S. Meyer, R. L. Shearer, E. E. Capowski, L. S. Wright, K. A. Wallace, E. L. McMillan, S.-C. Zhang, D. M. Gamm, *Proc. Natl. Acad. Sci. USA* **2009**, *106*, 16698.
- [5] C. B. Mellough, E. Sernagor, I. Moreno-Gimeno, D. H. W. Steel, M. Lako, *Stem Cells* **2012**, *30*, 673.
- [6] T. Nakano, S. Ando, N. Takata, M. Kawada, K. Muguruma, K. Sekiguchi, K. Saito, S. Yonemura, M. Eiraku, Y. Sasai, *Cell Stem Cell* **2012**, *10*, 771.
- [7] F. Osakada, H. Ikeda, Y. Sasai, M. Takahashi, *Nat. Protoc.* **2009**, *4*, 811.
- [8] S. Reichman, A. Terray, A. Slembrouck, C. Nanteau, G. Orieux, W. Habeler, E. F. Nandrot, J.-A. Sahel, C. Monville, O. Goureau, *Proc. Natl. Acad. Sci.* **2014**, *111*, 8518.
- [9] C. Boucherie, S. Mukherjee, E. Henckaerts, A. J. Thrasher, J. C. Sowden, R. R. Ali, *Stem Cells* **2012**, *31*, 408.
- [10] A. Gonzalez-Cordero, K. Kruczek, A. Naeem, M. Fernando, M. Kloc, J. Ribeiro, D. Goh, Y. Duran, S. J. I. Blackford, L. Abelleira-Hervas, R. D. Sampson, I. O. Shum, M. J. Branch, P. J. Gardner, J. C. Sowden, J. W. B. Bainbridge, A. J. Smith, E. L. West, R. A. Pearson, R. R. Ali, *Stem Cell Rep.* **2017**, *9*, 820.
- [11] S. A. Jayakody, A. Gonzalez-Cordero, R. R. Ali, R. A. Pearson, *Prog. Retin. Eye Res.* **2015**, *46*, 31.
- [12] A. O. Barnea-Cramer, W. Wang, S.-J. Lu, M. S. Singh, C. Luo, H. Huo, M. E. McClements, A. R. Barnard, R. E. MacLaren, R. Lanza, *Sci. Rep.* **2016**, *6*, 29784.
- [13] J. Lakowski, A. Gonzalez-Cordero, E. L. West, Y.-T. Han, E. Welby, A. Naeem, S. J. I. Blackford, J. W. B. Bainbridge, R. A. Pearson, R. R. Ali, J. C. Sowden, *Stem Cells* **2015**, *33*, 2469.
- [14] M. S. Mehat, V. Sundaram, C. Ripamonti, A. G. Robson, A. J. Smith, S. Borooah, M. Robinson, A. N. Rosenthal, W. Innes, R. G. Weleber, R. W. J. Lee, M. Crossland, G. S. Rubin, B. Dhillon, D. H. W. Steel, E. Anglade, R. P. Lanza, R. R. Ali, M. Michaelides, J. W. B. Bainbridge, *Ophthalmology* **2018**.
- [15] D. A. Lamba, A. McUsic, R. K. Hirata, P.-R. Wang, D. Russell, T. A. Reh, *PLoS ONE* **2010**, *5*, e8763.

- [16] B. A. Tucker, I.-H. Park, S. D. Qi, H. J. Klassen, C. Jiang, J. Yao, S. Redenti, G. Q. Daley, M. J. Young, *PLoS ONE* **2011**, *6*, e18992.
- [17] A. Gonzalez-Cordero, E. L. West, R. A. Pearson, Y. Duran, L. S. Carvalho, C. J. Chu, A. Naeem, S. J. I. Blackford, A. Georgiadis, J. Lakowski, M. Hubank, A. J. Smith, J. W. B. Bainbridge, J. C. Sowden, R. R. Ali, *Nat. Biotechnol.* **2013**, *31*, 741.
- [18] L. Zhou, W. Wang, Y. Liu, J. F. de Castro, T. Ezashi, B. P. V. L. Telugu, R. M. Roberts, H. J. Kaplan, D. C. Dean, *Stem Cells* **2011**, *29*, 972.
- [19] D. A. Thompson, R. R. Ali, E. Banin, K. E. Branham, J. G. Flannery, D. M. Gamm, W. W. Hauswirth, J. R. Heckenlively, A. Iannaccone, K. T. Jayasundera, N. W. Khan, R. S. Molday, M. E. Pennesi, T. A. Reh, R. G. Weleber, D. N. Zacks, *Invest. Ophthalmol. Vis. Sci.* **2015**, *56*, 918.
- [20] P. V. Waldron, F. Di Marco, K. Kruczek, J. Ribeiro, A. B. Graca, C. Hippert, N. D. Aghaizu, A. A. Kalargyrou, A. C. Barber, G. Grimaldi, Y. Duran, S. J. I. Blackford, M. Kloc, D. Goh, E. Z. Aldunate, R. D. Sampson, J. W. B. Bainbridge, A. J. Smith, A. Gonzalez-Cordero, J. C. Sowden, R. R. Ali, R. A. Pearson, *Stem Cell Rep.* **2018**, *10*, 406.
- [21] K. Achberger, J. C. Haderspeck, A. Kleger, S. Liebau, *Adv. Drug Deliv. Rev.* **2018**.
- [22] F. S. Veraitch, R. Scott, J.-W. Wong, G. J. Lye, C. Mason, *Biotechnol. Bioeng.* **2007**, *99*, 1216.
- [23] T. G. Fernandes, M. M. Diogo, *J. Chem. Technol. Biotechnol.* **2013**, *89*.
- [24] P. Ovando-Roche, E. L. West, M. J. Branch, R. D. Sampson, M. Fernando, P. Munro, A. Georgiadis, M. Rizzi, M. Kloc, A. Naeem, J. Ribeiro, A. J. Smith, A. Gonzalez-Cordero, R. R. Ali, *Stem Cell Res. Ther.* **2018**, *9*, 156.
- [25] M. P. Marques, N. Szita, *Curr. Opin. Chem. Eng.* **2017**, *18*, 61.
- [26] D. M. Titmarsh, H. Chen, N. R. Glass, J. J. Cooper-White, *Stem Cells Transl. Med.* **2013**, *3*, 81.
- [27] J. S. Jeon, S. Bersini, J. A. Whisler, M. B. Chen, G. Dubini, J. L. Charest, M. Moretti, R. D. Kamm, *Integr. Biol. (Camb)* **2014**, *6*, 555.
- [28] R. Yoshimitsu, K. Hattori, S. Sugiura, Y. Kondo, R. Yamada, S. Tachikawa, T. Satoh, A. Kurisaki, K. Ohnuma, M. Asashima, T. Kanamori, *Biotechnol. Bioeng.* **2013**, *111*, 937.
- [29] E. Cimetta, D. Sirabella, K. Yeager, K. Davidson, J. Simon, R. T. Moon, G. Vunjak-Novakovic, *Lab. Chip.* **2012**, *13*, 355.
- [30] B.-Y. Xu, S.-W. Hu, G.-S. Qian, J.-J. Xu, H.-Y. Chen, *Lab. Chip.* **2013**, *13*, 3714.
- [31] M. Hemmingsen, S. Vedel, P. Skafto-Pedersen, D. Sabourin, P. Collas, H. Bruus, M. Dufva, *PLoS ONE* **2013**, *8*, e63638.
- [32] A. Tourovskaia, X. Figueroa-Masot, A. Folch, *Lab. Chip.* **2004**, *5*, 14.
- [33] M. Reichen, R. J. Macown, N. Jaccard, A. Super, L. Ruban, L. D. Griffin, F. S. Veraitch, N. Szita, *PLoS ONE* **2012**, *7*, e52246.
- [34] R. J. Macown, F. S. Veraitch, N. Szita, *Biotechnol. J.* **2014**, *9*, 805.
- [35] A. Super, N. Jaccard, M. P. C. Marques, R. J. Macown, L. D. Griffin, F. S. Veraitch, N. Szita, *Biotechnol. J.* **2016**, *11*, 1179.
- [36] K. Mehta, J. J. Linderman, *Biotechnol. Bioeng.* **2006**, *94*, 596.
- [37] K. Katoh, Y. Omori, A. Onishi, S. Sato, M. Kondo, T. Furukawa, *J. Neurosci.* **2010**, *30*, 6515.
- [38] S. Llonch, M. Carido, M. Ader, *Dev. Biol.* **2017**, *433*, 132.
- [39] Y.-C. Toh, J. Voldman, *FASEB J.* **2010**, *25*, 1208.
- [40] E. M. Pera, O. Wessely, S. Y. Li, E. M. De Robertis, *Dev. Cell.* **2001**, *1*, 655.
- [41] D. J. Horsford, M.-T. T. Nguyen, G. C. Sellar, R. Kothary, H. Arnheiter, R. R. McInnes, *Development* **2004**, *132*, 177.
- [42] T. Furukawa, S. Mukherjee, Z.-Z. Bao, E. M. Morrow, C. L. Cepko, *Neuron* **2000**, *26*, 383.
- [43] A. J. Mears, M. Kondo, P. K. Swain, Y. Takada, R. A. Bush, T. L. Saunders, P. A. Sieving, A. Swaroop, *Nature Genetics* **2001**, *29*, 447.